






## ORIGINAL ARTICLE

OPEN

# ALK1 controls hepatic vessel formation, angiodiversity, and angiocrine functions in hereditary hemorrhagic telangiectasia of the liver

Christian David Schmid<sup>1,2</sup>  | Victor Olsavszky<sup>1,2</sup>  | Manuel Reinhart<sup>1,2</sup> |  
 Vanessa Weyer<sup>3,4</sup> | Felix A. Trogisch<sup>2,5,6</sup> | Carsten Sticht<sup>7</sup> |  
 Manuel Winkler<sup>1,2</sup>  | Sina W. Kürschner<sup>1,2</sup> | Johannes Hoffmann<sup>1,2</sup>  |  
 Roxana Ola<sup>8</sup> | Theresa Staniczek<sup>1,2</sup> | Joerg Heineke<sup>2,5,6</sup> | Beate K. Straub<sup>9</sup> |  
 Jens Mittler<sup>10</sup> | Kai Schledzewski<sup>1,2</sup> | Peter ten Dijke<sup>11</sup> | Karsten Richter<sup>12</sup> |  
 Steven Dooley<sup>13</sup> | Cyrill Géraud<sup>1,14</sup> | Sergij Goerdts<sup>1</sup> | Philipp-Sebastian Koch<sup>1</sup> 

<sup>1</sup>Department of Dermatology, Venereology and Allergology, University Medical Center and Medical Faculty Mannheim, Heidelberg University, Mannheim, Germany

<sup>2</sup>European Center for Angioscience, Medical Faculty Mannheim, Heidelberg University, Mannheim, Germany

<sup>3</sup>Department of Neuroradiology, University Medical Center and Medical Faculty Mannheim, Heidelberg University, Mannheim, Germany

<sup>4</sup>Department of Radiation Oncology, University Medical Center and Medical Faculty Mannheim, Heidelberg University, Mannheim, Germany

<sup>5</sup>Department of Cardiovascular Physiology, Medical Faculty Mannheim, Heidelberg University, Mannheim, Germany

<sup>6</sup>DZHK (German Center for Cardiovascular Research), partner site Heidelberg/Mannheim, Mannheim, Germany

<sup>7</sup>Core Facility Platform Mannheim, NGS Core Facility, Medical Faculty Mannheim, Heidelberg University, Mannheim, Germany

<sup>8</sup>Department of Cardiovascular Pharmacology, Medical Faculty Mannheim, Heidelberg University, Mannheim, Germany

<sup>9</sup>Institute of Pathology, University Medical Center of the Johannes Gutenberg-University Mainz, Mainz, Germany

<sup>10</sup>Department of General, Visceral, and Transplant Surgery, University Medical Center of the Johannes Gutenberg-University Mainz, Mainz, Germany

<sup>11</sup>Oncode Institute, Department of Cell and Chemical Biology, Leiden University Medical Center, Leiden, The Netherlands

<sup>12</sup>Division of Molecular Genetics, German Cancer Research Center (DKFZ), Heidelberg, Germany

<sup>13</sup>Department of Medicine II, University Medical Center Mannheim, Medical Faculty Mannheim, Heidelberg University, Mannheim, Germany

<sup>14</sup>Section of Clinical and Molecular Dermatology, Department of Dermatology, Venereology and Allergology, University Medical Center and Medical Faculty Mannheim, Heidelberg University, Mannheim, Germany

**Abbreviations:** Acvr11, activin A receptor-like type 1; Alk1, activin receptor-like kinase 1; Apln, apelin; BMP, bone morphogenetic protein; CT, computed tomography; ECM, extracellular matrix; EMCN, endomucin; GLUL, glutamine synthetase; GSEA, gene set enrichment analysis; HEC-KO, hepatic endothelial knockout; HHT, hereditary hemorrhagic telangiectasia; iCreF3, codon-improved cre recombinase founder 3; ID, inhibitor of DNA binding; ISH, in situ hybridization; LSEC, liver sinusoidal endothelial cells; LYVE-1, lymphatic vessel endothelial hyaluronan receptor 1; PGF, placental growth factor; PRND, prion-like protein doppel; qPCR, quantitative polymerase chain reaction; RNA-seq, RNA-sequencing; Rspo3, R-spondin-3; Stab2, stabilin-2; VEGF, vascular endothelial growth factor; VEGFR, vascular endothelial growth factor receptor; Wnt, portmanteau of the names Wingless and Int-1;  $\alpha$ -SMA, alpha smooth muscle actin.

Christian David Schmid, Victor Olsavszky, and Manuel Reinhart contributed equally to this work and share first authorship.

Sergij Goerdts and Philipp-Sebastian Koch contributed equally to this work and share last authorship.

Supplemental Digital Content is available for this article. Direct URL citations appear in the printed text and are provided in the HTML and PDF versions of this article on the journal's website, [www.hepjournal.com](http://www.hepjournal.com).

This is an open access article distributed under the terms of the Creative Commons Attribution-Non Commercial-No Derivatives License 4.0 (CCBY-NC-ND), where it is permissible to download and share the work provided it is properly cited. The work cannot be changed in any way or used commercially without permission from the journal.

Copyright © 2023 The Author(s). Published by Wolters Kluwer Health, Inc.

**Correspondence**

Victor Olsavszky, Department of Dermatology, Venereology and Allergology, University Medical Center and Medical Faculty Mannheim, Heidelberg University, Theodor-Kutzer-Ufer 1-3, 68167 Mannheim, Germany. Email: [victor.olsavszky@umm.de](mailto:victor.olsavszky@umm.de)

**Funding information**

Deutsche Forschungsgemeinschaft, Grant/Award Number: 259332240 - RTG/GRK 2099, 314905040 - CRC/SFB-TR 209, 394046768 - CRC/SFB 1366 and 413262200 - ICON/EB 187/8-1; Ministry of Science, Research and the Arts Baden-Württemberg (MWK) and Deutsche Forschungsgemeinschaft, Grant/Award Number: INST35/1314-1FUGG

**Abstract**

**Background and Aims:** In hereditary hemorrhagic telangiectasia (HHT), severe liver vascular malformations are associated with mutations in the Activin A Receptor-Like Type 1 (*ACVRL1*) gene encoding ALK1, the receptor for bone morphogenetic protein (BMP) 9/BMP10, which regulates blood vessel development. Here, we established an HHT mouse model with exclusive liver involvement and adequate life expectancy to investigate ALK1 signaling in liver vessel formation and metabolic function.

**Approach and Results:** Liver sinusoidal endothelial cell (LSEC)-selective Cre deleter line, *Stab2-iCreF3*, was crossed with *Acvrl1*-floxed mice to generate LSEC-specific *Acvrl1*-deficient mice (*Alk1<sup>HEC-KO</sup>*). *Alk1<sup>HEC-KO</sup>* mice revealed hepatic vascular malformations and increased posthepatic flow, causing right ventricular volume overload. Transcriptomic analyses demonstrated induction of proangiogenic/tip cell gene sets and arterialization of hepatic vessels at the expense of LSEC and central venous identities. Loss of LSEC angiokines *Wnt2*, *Wnt9b*, and R-spondin-3 (*Rspo3*) led to disruption of metabolic liver zonation in *Alk1<sup>HEC-KO</sup>* mice and in liver specimens of patients with HHT. Furthermore, prion-like protein doppel (*Pmd*) and placental growth factor (*Pgf*) were upregulated in *Alk1<sup>HEC-KO</sup>* hepatic endothelial cells, representing candidates driving the organ-specific pathogenesis of HHT. In LSEC *in vitro*, stimulation or inhibition of ALK1 signaling counter-regulated Inhibitors of DNA binding (ID)1–3, known Alk1 transcriptional targets. Stimulation of ALK1 signaling and inhibition of ID1–3 function confirmed regulation of *Wnt2* and *Rspo3* by the BMP9/ALK1/ID axis.

**Conclusions:** Hepatic endothelial ALK1 signaling protects from development of vascular malformations preserving organ-specific endothelial differentiation and angiocrine signaling. The long-term surviving *Alk1<sup>HEC-KO</sup>* HHT model offers opportunities to develop targeted therapies for this severe disease.

**INTRODUCTION**

Hereditary hemorrhagic telangiectasia (HHT) is an autosomal dominant genetic disease that causes vascular malformations in multiple organs. The most common symptoms of HHT are epistaxis, telangiectases, and visceral lesions.<sup>[1]</sup> HHT has a low prevalence of 1:5000 and, therefore, the diagnosis is often made with a delay of many years.<sup>[2]</sup> Recurrent epistaxis affects about 90% of patients with HHT and represents the most frequent and obvious complaint.<sup>[3]</sup> However, malformations and shunts in internal organs, such as the liver, are more relevant for the long-term prognosis as they can ultimately lead to heart failure.<sup>[4]</sup>

Genetic loss-of-function mutations of *ENG* (encoding Endoglin) or *ACVRL1* (encoding activin receptor-like kinase 1 [ALK1]) distinguish the two subtypes of HHT,

i.e., HHT1 and HHT2.<sup>[5,6]</sup> In HHT1, visceral vascular malformations are predominantly found in the brain and lungs, whereas *ACVRL1* mutations in HHT2 are frequently associated with vascular malformations in the liver.<sup>[7]</sup> ALK1 and Endoglin are involved in angiogenesis, in which ALK1 drives the stalk cell phenotype in cooperation with Notch signaling, whereas tip cells exhibit only minor ALK1 activity.<sup>[8]</sup>

Both Endoglin and ALK1 are members of the same branch of the transforming growth factor beta signaling superfamily that also comprises bone morphogenetic protein (BMP)-9, BMP-10, and SMAD4.<sup>[9]</sup> In the liver, BMP-9 is primarily secreted by hepatic stellate cells,<sup>[10,11]</sup> binds to the endothelial ALK1-Endoglin receptor complex,<sup>[12,13]</sup> and activates the SMAD1/5/8-SMAD4 signal transduction pathway to regulate gene expression programs.<sup>[14]</sup> ALK1-dependent BMP-9

signaling is supposed to play a role in hepatic fibrogenesis. So far, however, it is not fully established under which conditions BMP-9 signaling in liver sinusoidal endothelial cells (LSEC) acts to promote or prevent hepatic fibrogenesis.<sup>[11,15]</sup> This issue is further complicated by the fact that hepatic fibrogenesis has been shown to depend on the genetic background in the respective preclinical models.<sup>[16]</sup>

Investigating HHT and ALK1 signaling in preclinical models is challenging due to the high mortality that has been observed. Therefore, most preclinical models have to be used at very early time points after HHT induction, and *ex vivo* systems such as the retina are preferred. Notably, vascular malformations of the liver are not covered well by currently available mouse models.<sup>[17]</sup>

The vascular system of the liver is highly complex featuring hepatic arteries and veins, portal vessels, and a special microvascular bed, i.e., the hepatic sinusoids. The hepatic sinusoids are lined by LSEC, a discontinuous variety of endothelial cells (EC) featuring wide transcellular pores called fenestrae.<sup>[18]</sup> LSEC lack a continuous basement membrane, but they are embedded in extracellular matrix (ECM) proteins in the space of Disse that extends from the abluminal side of LSEC to the luminal pole of hepatocytes. LSEC are not only morphologically distinct EC, but they exert specialized functions in regulating liver immunity and inflammation, and by clearing a variety of blood factors from the circulation via endocytic receptors, such as the mannose receptor, CD32b, lymphatic vessel endothelial hyaluronan receptor 1 (LYVE-1), Stabilin-1, and Stabilin-2 (Stab2). In addition, the microvascular niche of the liver sinusoids comprises Kupffer cells, i.e., sinusoidal macrophages, and hepatic stellate cells, which store vitamin A and may transdifferentiate upon liver injury to myofibroblasts, developing a cytoskeleton rich in alpha smooth muscle actin (ACTA2).<sup>[19]</sup>

With its dual blood supply and its highly specialized sinusoidal microvascular niche, the liver vasculature represents a paradigm of organotypic and segmental angiodiversity.<sup>[20,21]</sup> Previously, we have shown that microvascular angiodiversity in the liver depends on a special LSEC differentiation program controlled by transcription factor GATA-4. GATA-4-dependent organ-specific endothelial differentiation controls liver development and embryonic hematopoiesis.<sup>[22]</sup> In the adult liver, LSEC control liver function and hepatic fibrogenesis by paracrine signaling via organotypic angiocrine factors.<sup>[23]</sup> In particular, loss of portmanteau of the names Wingless and Int-1 (Wnt) factors disrupts metabolic liver zonation, whereas *de novo* expression of endothelial platelet-derived growth factor (PDGF) promotes stellate cell activation and fibrogenesis upon endothelial GATA-4 deficiency in the adult liver. Within the hepatic vascular niche, however, the role of endothelial ALK1 signaling has not yet been comprehensively analyzed.

Here, we established a preclinical genetic HHT model featuring exclusive hepatic involvement and adequate life expectancy. Hepatic EC-specific *Alk1* deficiency caused development of massive hepatic vascular malformations and of shunting with increased blood flow as well as disruption of metabolic liver zonation. The organ-specific GATA-4-dependent vascular differentiation program was overruled by activation of angiogenesis and arterialization. Notably, we identified Prion-Like Protein Doppel (PRND) and placental growth factor (PGF) as angiogenic molecules in the pathogenesis of HHT, indicating that ALK1 may inhibit an autocrine angiogenic feedforward loop in organotypic EC in the liver. In general, our data suggest that endothelial ALK1 signaling maintains vascular quiescence in the liver without compromising endothelial differentiation programs that generate and control organotypic angiodiversity and vascular heterogeneity along the different segments of the vascular tree. As a long-term surviving preclinical HHT model, the *Alk1*<sup>HEC-KO</sup> mouse line constitutes a powerful tool for analyzing the *in vivo* functions of hepatic endothelial ALK1 signaling, and it may also be used to develop and test targeted therapies for HHT.

## PATIENTS AND METHODS

### Ethical compliance

The experimental protocols used in this study complied with national and international ethical guidelines and, in case of animal models, were approved by the animal welfare commission of the Regierungspräsidium Karlsruhe (Karlsruhe, Germany).

### Patients and controls

Each four liver samples of healthy individuals and those with HHT were provided by and in accordance with the regulations of the Tissue Biobank of the University Medical Center Mainz after approval by the local ethics committee (Ethik-Kommission der Landesärztekammer Rheinland-Pfalz, 837.146.17 [10980], as well as addendum 2018-13857\_1 and 2021-16,239 to B.K.S.). All experiments were carried out in accordance with the Declaration of Helsinki.<sup>[24]</sup>

### Animal models

Female and male mice aged 1 to 12 months were used in this study. Mice were housed under specific pathogen-free conditions in single ventilated cages in a 12 h/12 h day/night cycle and fed *ad libitum* with a standard

rodent diet (V1534-000, Ssniff) with free access to water.

For the generation of hepatic endothelial conditional *Acvr11*-knockout mice, *Stab2-icreF3* mice (C57BL/6N-Tg [*Stab2-icre*]1.3Cger/Sgoe, Mouse Genome Informatics [MGI]: 6741034)<sup>[25]</sup> were crossed with *Acvr11*-floxed mice (B6N.129-*Acvr11*<sup>tm2.1Spo</sup>, MGI: 4398901).<sup>[26]</sup> Mice with the genotype *Stab2-icreF3*<sup>tg/wt</sup> × *Acvr11*<sup>fl/fl</sup> indicating homozygous recombination were denoted as *Alk1*<sup>HEC-KO</sup> (alias *Acvr11*<sup>HEC-KO</sup>). Littermates with the genotypes *Stab2-icreF3*<sup>wt/wt</sup> × *Alk1*<sup>fl/fl</sup> or *Stab2-icreF3*<sup>wt/wt</sup> × *Alk1*<sup>fl/wt</sup> were used as controls. *Alk1* knockout was confirmed by RNA-sequencing (RNA-seq) of isolated hepatic EC and by immunofluorescence of ALK1 target Endoglin.

## Statistical analysis

Statistical analyses were conducted in R 3.6.1 (R Core Team), Prism 8 (GraphPad Software), or JMP 15.2.1 (SAS Institute). For sample size calculation, we suggested an  $\alpha$ -level of 0.05 and a  $\beta$ -level of 0.2, whereas the power was adjusted for each experiment. Welch's *t* test, Mann–Whitney *U* test, and Fisher's exact test were used for statistical testing. A *p* value of <0.05 was considered statistically significant. The appropriate statistical test was chosen according to the requirements of each test (e.g., normal distribution). Normal distribution was assessed using the Shapiro–Wilk test.

## Additional methodological details

For further information on materials and methods, please refer to the [Supporting Data](#).

## RESULTS

### Adult *Alk1*<sup>HEC-KO</sup> mice exhibit macroscopic hepatic vascular malformations

To investigate the pathophysiology of HHT in the liver, we generated a mouse model with hepatic endothelial *Alk1* deficiency. *Stab2*-promotor–controlled iCre-mice (*Stab2-iCreF3*)<sup>[25]</sup> were crossed with mice exhibiting a floxed *Acvr11* (*Alk1*) gene.<sup>[26]</sup> *Stab2-icreF3*<sup>tg/wt</sup> × *Acvr11*<sup>fl/fl</sup> (*Alk1*<sup>HEC-KO</sup>) mice showed a median life expectancy of 46 weeks and thus represent a valuable tool for HHT research (Figure S1A).

To assess the large hepatic vessels in 3-month-old *Alk1*<sup>HEC-KO</sup> mice, we performed computed tomography (CT) with a contrast medium (ExiTron nano 6000) that is taken up by Kupffer cells of the liver resulting in long-term x-ray contrast. The basic liver vessel anatomy was conserved in *Alk1*<sup>HEC-KO</sup> mice (Figure 1A); however, CT

images showed diffuse parenchymal heterogeneity and numerous telangiectasias. The normalized area of detectable intrahepatic large vessels was significantly increased in *Alk1*<sup>HEC-KO</sup> mice (Figure 1A,B). Measuring the diameters of the main hepatic vessels, we found that the diameters of the portal vein and most of its branches as well as the hepatic artery were not significantly affected compared to controls (Figure S1B–D). Moreover, there were no differences in portal blood flow between *Alk1*<sup>HEC-KO</sup> and control mice (Figure S1E), indicating absence of portal hypertension. In contrast, the hepatic veins of *Alk1*<sup>HEC-KO</sup> mice were significantly enlarged (Figure 1C), resulting in dilation of the vena cava beyond the confluence of hepatic veins (Figure 2A). Dilation of the hepatic veins and the vena cava indicates enhanced hepatic blood flow and represents a surrogate parameter for functional shunting of vessels within the liver.

### Increased posthepatic vena cava flow entails volume overload of the right ventricle in *Alk1*<sup>HEC-KO</sup> mice

As we observed dilation of the posthepatic vena cava in *Alk1*<sup>HEC-KO</sup> mice by CT imaging, we examined vena cava blood flow using Doppler ultrasonography in 6-month-old mice. Blood flow in the posthepatic vena cava of *Alk1*<sup>HEC-KO</sup> mice was significantly increased as compared to controls, whereas the prehepatic vena cava was unaltered (Figure 2B–D), yielding an increased post/prehepatic vessel flow gradient (Figure 2E). Color-coded Doppler analyses of the liver confirmed the increase in large vessels within the liver parenchyma (Figure S2). Altogether, our data confirm functional shunting in the liver of *Alk1*<sup>HEC-KO</sup> mice.

To investigate whether hepatic malformations and increased vena cava flow affect cardiac function in *Alk1*<sup>HEC-KO</sup> mice, we performed echocardiography of 6-month-old animals. Both the right ventricular systolic area and the right ventricular diastolic area were significantly increased in *Alk1*<sup>HEC-KO</sup> mice, whereas the right ventricular fractional area change was not affected (Figure S3A–D). On the contrary, the left ventricular systolic area, the left ventricular diastolic area, and the left ventricular fractional area change as well as the heart rate were not significantly altered in *Alk1*<sup>HEC-KO</sup> mice (Figure S3E–J). In conclusion, these findings indicate volume overload of the right heart with preserved right heart function in *Alk1*<sup>HEC-KO</sup> mice.

### Abnormal hepatic vascular differentiation in *Alk1*<sup>HEC-KO</sup> mice

We sacrificed 3-month-old *Alk1*<sup>HEC-KO</sup> mice to dissect histological changes upon hepatic *Alk1* deficiency.

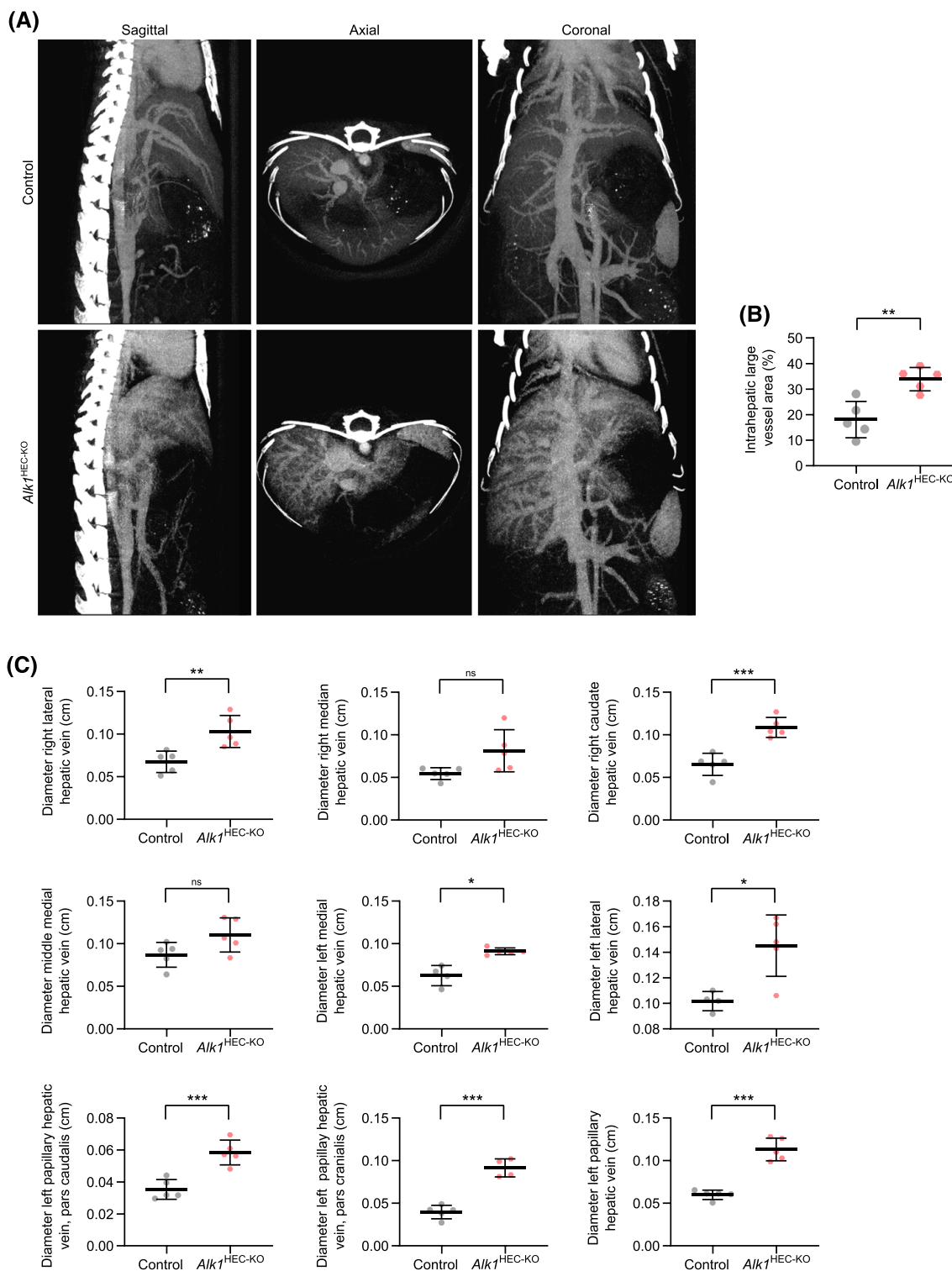


**FIGURE 1** *Alk1*<sup>HEC-KO</sup> mice exhibit a vascular parenchymal enhancement and dilated hepatic veins. (A) Computed tomography sections in sagittal, axial, and coronal planes ( $n = 5$ ). (B) Quantification of intrahepatic large vessel density in (A) ( $n = 5$ ). (C) Diameters of hepatic vein branches ( $n \geq 4$ ). Error bars: Mean with standard deviation. (B,C) Welch's  $t$  test. \* $p < 0.05$ ; \*\* $p < 0.01$ ; \*\*\* $p < 0.001$ .

Macroscopically, livers from *Alk1*-deficient mice exhibited small but dilated superficial blood vessels, whereas the liver surface did not reveal signs of liver fibrosis (Figure 3). Moreover, the liver-to-body-weight ratio was not altered in *Alk1*<sup>HEC-KO</sup> mice (Table S1). Microscopically, the central

veins were dilated in *Alk1*<sup>HEC-KO</sup> mice, whereas we did not notice necrotic areas or fibrosis upon hematoxylin and eosin or Sirius Red staining, respectively (Figure 3B). Notably, dilatation of hepatic vessels evolved during maturation, i.e., dilatation was minimal in 1-month-old

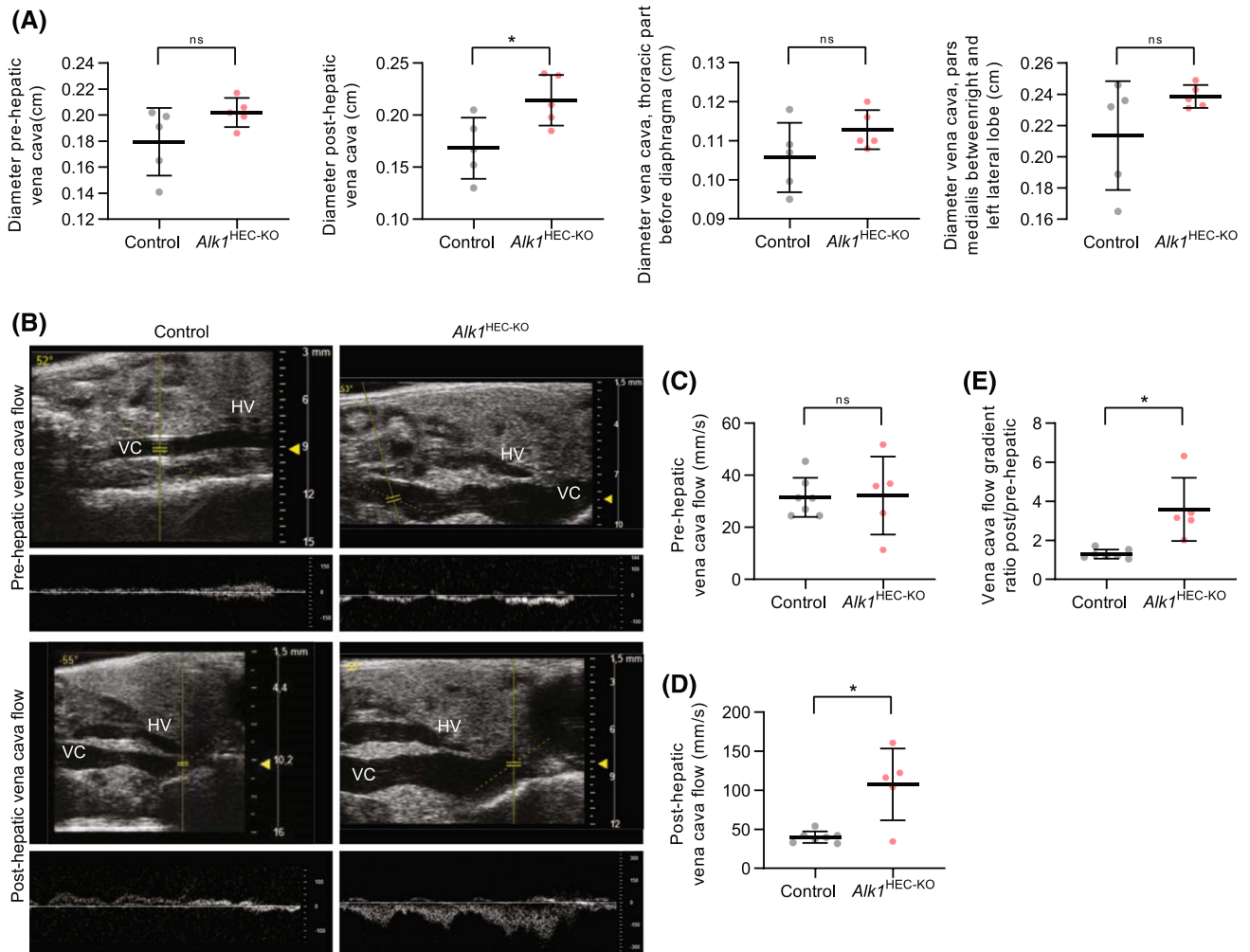


**FIGURE 2** Posthepatic volume overload of the vena cava in *Alk1*<sup>HEC-KO</sup> mice. (A) Diameters of vena cava segments ( $n = 5$ ). (B) Doppler sonography of vena cava before and after confluence of hepatic veins ( $n \geq 5$ ). (C–E) Blood flow velocity in vena cava before and after confluence of hepatic veins ( $n \geq 5$ ). HV, hepatic vein; VC, vena cava. Error bars: Mean with standard deviation. (A, C–E) Welch's  $t$  test. \* $p < 0.05$ .

mice (Figure S4A), whereas the degree of vascular dilatation was similar in 3-month-old and in 6-month-old mice (Figure 3B, Figure S4B). On the contrary, neither necrotic areas nor fibrotic changes developed in older animals (Figure S4A,B). Basic plasma parameters revealed no fundamental alterations, and liver function tests were largely normal (Table S1).

Upon immunohistochemical analysis, we noticed loss of Endoglin, a coreceptor of ALK1 and target gene of ALK1 signal transduction, indicating loss of ALK1 function in *Alk1*<sup>HEC-KO</sup> mice (Figure 3C). Notably, the hepatic vascular structures in *Alk1*<sup>HEC-KO</sup> mice appeared irregular and distended. Overall, an increase of continuous endothelial marker endomucin (EMCN) was seen, whereas LSEC marker LYVE-1 was reduced (Figure 3C). Regarding ECM molecules, we could not detect altered deposition of COL4A1 along the hepatic sinusoids in *Alk1*<sup>HEC-KO</sup> mice; however, COL4A1 staining highlighted distorted, slit-like sinusoids (Figure S5A,B). Expression of LAMC1 and COL18A1 was significantly enhanced in the space of Disse in the

livers of 3-month-old *Alk1*<sup>HEC-KO</sup> mice (Figure S5A–D). In the livers of 6-month-old *Alk1*<sup>HEC-KO</sup> mice, perisinusoidal expression of LAMC1 was enhanced in three out of four mice with one outlier showing the same level of expression as the controls, accounting altogether for the statistically nonsignificant results. Perisinusoidal COL18A1 was significantly enhanced regarding fluorescence intensity but not area stained (Figure S5A–D). Transmission electron microscopy revealed local thickening of LSEC and focal deposition of amorphous collagenous material in the space of Disse in the livers of *Alk1*<sup>HEC-KO</sup> mice, whereas sparsely distributed discrete collagen bundles were found in the space of Disse in both *Alk1*<sup>HEC-KO</sup> and control mice. Throughout the sinusoidal network, fenestrations were preserved and a continuous basal lamina did not develop beneath the LSEC cell layer (Figure S5E), indicating aberrant sinusoidal differentiation, but not full capillarization. In addition, we observed LYVE-1-positive, thin-walled, elongated vessels that were negative for blood vascular endothelial markers CD31 or EMCN and thus seemed

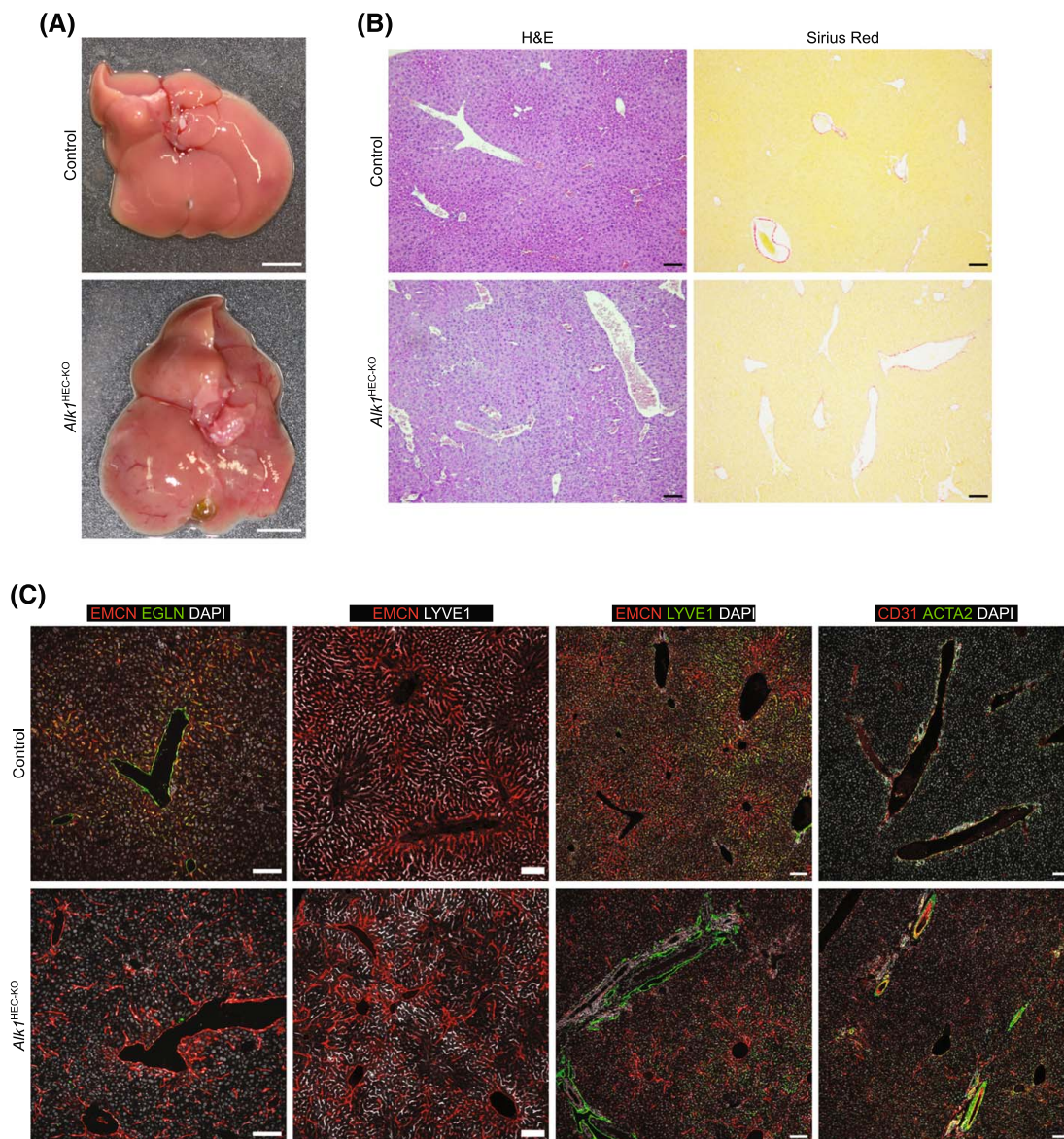


**FIGURE 3** *Alk1* deficiency causes disturbed hepatic vessel architecture. (A) Macroscopic images of livers ( $n \geq 7$ ). (B) Hematoxylin and eosin (H&E) and Sirius Red staining of livers ( $n \geq 7$ ). (C) Immunofluorescence staining of livers for Endomucin (EMCN) and Endoglin, EMCN and lymphatic vessel endothelial hyaluronan receptor 1 (LYVE-1), and CD31 and alpha-SMA (ACTA2) ( $n = 5$ ). (A) Scale bar: 5 mm; (B,C) scale bars: 100  $\mu$ m.

to represent lymphatic vessels (Figure 3C). Furthermore, *Alk1*-deficient mice exhibited numerous  $\alpha$ -SMA (ACTA)-positive large vessels, i.e., arteries and veins, within the liver parenchyma (Figure 3C).

### Hepatic EC undergo arterialization in *Alk1*<sup>HEC-KO</sup> mice

To reveal the underlying transcriptomic alterations in hepatic EC of *Alk1*-deficient mice, we isolated hepatic EC of 3-month-old *Alk1*<sup>HEC-KO</sup> mice and subsequently performed bulk RNA-seq. Hierarchical clustering and principal component analysis revealed good reproducibility for all five samples within the two groups of hepatic

EC from *Alk1*<sup>HEC-KO</sup> and control mice (Figure S6A). Exon-specific analysis of the *Acvr11* locus demonstrated successful recombination of exons 4 to 6, confirming *Alk1* deficiency in hepatic EC (Figure S6B,C).

Using the processed data, 1369 genes were significantly downregulated, whereas 1596 genes were significantly upregulated using a false discovery rate (FDR) cutoff of 0.05 (Figure 4A). We used hepatic endothelial gene sets identified by single cell RNA-seq<sup>[27]</sup> to decipher differentiation of EC in *Alk1*<sup>HEC-KO</sup> mice. Hepatic EC differentiation shifted from sinusoidal, i.e., LSEC, and capillary venous, i.e., central vein, as well as large vein differentiation toward capillary arterial and large arterial differentiation in *Alk1*<sup>HEC-KO</sup> mice (Figure 4A). Besides, genes defining lymphatic EC were upregulated upon *Alk1*

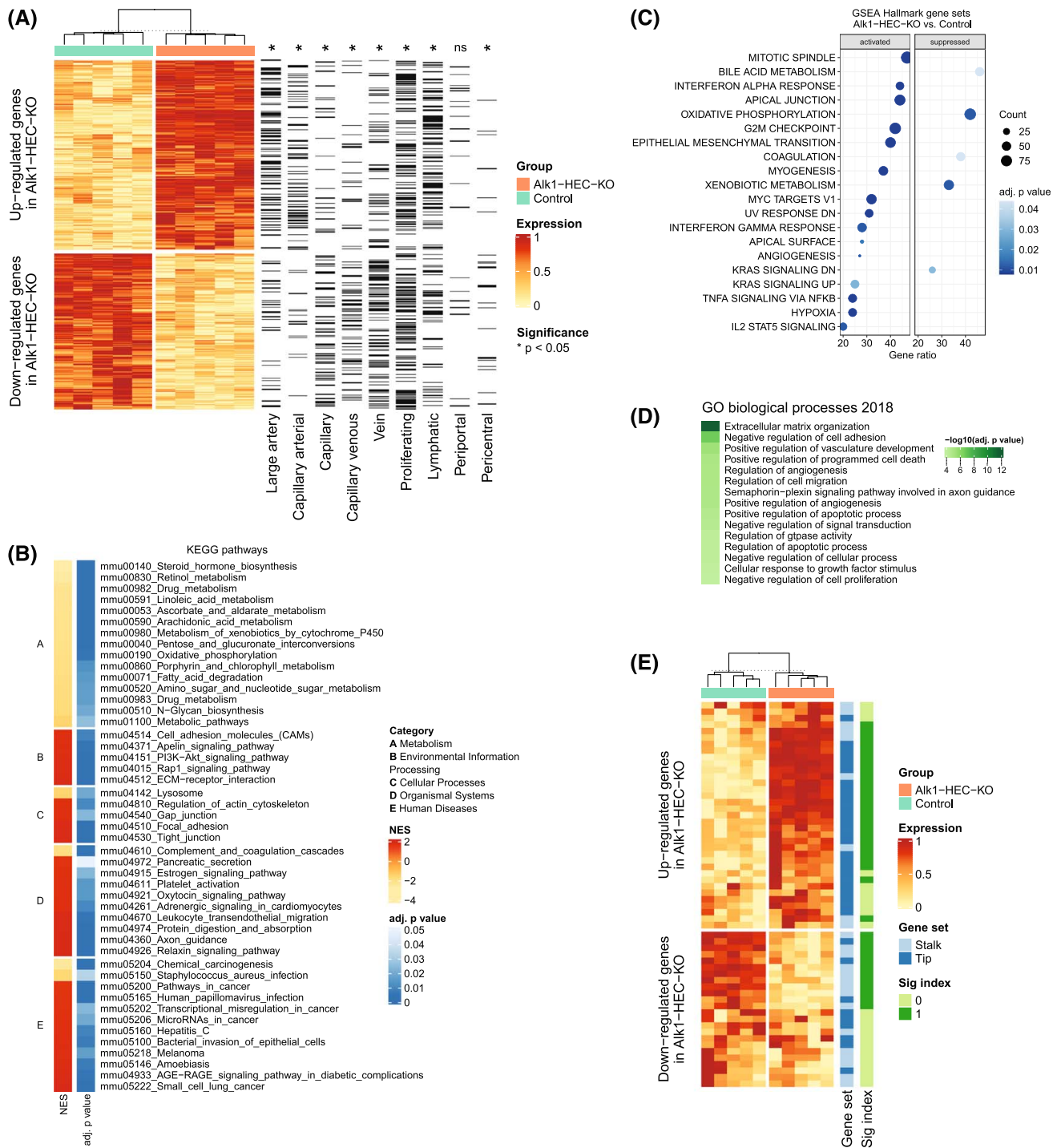


**FIGURE 4** Arterialization of hepatic vessels and loss of pericentral genes in *Alk1*<sup>HEC-KO</sup> mice. (A) Heatmap of significantly regulated genes in RNA-sequencing (RNA-seq) data of hepatic endothelial cells with annotation for gene sets from Kalucka et al.<sup>[27]</sup> and Halpern et al.<sup>[28]</sup> ( $n = 5$ ). (B, C) Gene set enrichment analysis (GSEA) of RNA-seq data using (B) the Kyoto Encyclopedia of Genes and Genomes (KEGG) database ( $n = 5$ ) and (C) Molecular Signatures Database (MSigDB) hallmark gene sets ( $n = 5$ ). (D) Overrepresentation analysis (ORA) for significantly regulated genes using the Gene Ontology biological processes gene sets ( $n = 5$ ). (E) Heatmap for stalk- and tip cells marker genes<sup>[30]</sup> with annotation of significance in RNA-seq data of hepatic endothelial cells from *Alk1*<sup>HEC-KO</sup> mice ( $n = 5$ ).

deficiency, confirming our observation of excessive lymphatic vessels seen upon immunofluorescence (Figure 4A). To independently confirm these findings, we also employed periportal and pericentral endothelial gene sets identified by single cell RNA-seq.<sup>[28]</sup> As expected, the

pericentral endothelial gene set was significantly reduced in *Alk1*<sup>HEC-KO</sup> mice, whereas the periportal endothelial gene set was upregulated, indicating that hepatic endothelial zonation was impaired at the expense of LSEC and central venous identities (Figure 4A).



## Alk1 deficiency activates proangiogenic pathways in hepatic EC

Next, we performed unbiased gene set enrichment analyses (GSEA) to identify pathways and biological processes controlled by ALK1 signaling in the liver vasculature. Enrichment for the Kyoto Encyclopedia of Genes and Genomes pathways yielded significant (FDR < 0.05) enrichment of 47 gene sets (Figure 4B). Among these, all 15 gene sets belonging to the metabolism category were downregulated, indicating a fundamental transformation in basic EC metabolism (Figure 4B). Notably, carbohydrate, amino acid, and fat metabolism were affected (Figure 4B).

The angiogenesis-related pathways Apelin (Apln)- and Phosphoinositide 3-kinase (PI3K)-Akt-signaling were found among the five significant gene sets of the environmental information processing category (Figure 4B), which is in line with data from Ola et al., who showed that *Alk1* deletion in human umbilical vein EC induced PI3K signaling.<sup>[29]</sup> Furthermore, we used the hallmark gene sets from Molecular Signatures Database for GSEA (Figure 4C). Among the most strongly regulated gene sets, we identified mitotic spindle genes, Myc targets, and angiogenesis as interesting gene sets that are linked with cell proliferation (Figure 4C). Overrepresentation of significantly regulated genes in *Alk1*<sup>HEC-KO</sup> mice using the Gene Ontology library revealed gene sets that comprised ECM organization, vascular development, and, again, angiogenesis (Figure 4D).

## Alk1 deficiency supports a proangiogenic tip cell phenotype in hepatic EC

Because we found angiogenesis among the activated gene sets in *Alk1*<sup>HEC-KO</sup> mice, we asked whether loss of *Alk1* favors tip or stalk cell identity in hepatic EC. To this end, we used tip and stalk cell phenotype genes<sup>[30]</sup> and analyzed these gene sets in liver endothelial *Alk1*<sup>HEC-KO</sup> RNA-seq data. Interestingly, about 65% of all genes belonging to either gene set were significantly regulated, indicating a major effect of *Alk1* deficiency on genes regulated during angiogenesis (Figure 4E). Comparing stalk cell and tip cell genes, tip cell genes were enriched in *Alk1*<sup>HEC-KO</sup> hepatic EC, whereas expression of stalk cell genes was reduced (Figure 4E). *Apln* and *Esm1*, two well-established tip cells markers, showed de novo expression in *Alk1*<sup>HEC-KO</sup> liver samples and colocalized with *Cdh5*-positive liver EC (Figure S7A,B). These findings were further supported by quantitative polymerase chain reaction (qPCR) analysis of isolated LSEC (Figure S7C). Thus, our data confirm the concept that ALK1 is necessary to support stalk cell differentiation during the transition from angiogenesis to vascular quiescence.<sup>[31]</sup>

## Proangiogenic angiocrine signaling in *Alk1*<sup>HEC-KO</sup> mice

Focusing on the 20 most strongly up- and down-regulated genes in EC from *Alk1*<sup>HEC-KO</sup> mice, we identified *Prnd* and *Pgf* as angiocrine, proangiogenic candidate genes (Figure 5A). qPCR validated the significant upregulation of *Prnd* and *Pgf* in hepatic EC with *Alk1* deficiency (Figure 5B). In situ hybridization (ISH) confirmed de novo expression of *Prnd* and *Pgf* in *Alk1*-deficient hepatic EC in liver tissue (Figure 5C,D), and fluorescent ISH revealed colocalization of *Prnd* and *Pgf* with *Cdh5*-positive liver EC (Figure 5E). Notably, placental growth factor 2, the secreted protein originating from the *Pgf* gene, showed significantly elevated plasma levels in *Alk1*<sup>HEC-KO</sup> mice as measured by enzyme-linked immunosorbent assay (Figure 5F).

## Metabolic liver zonation is disrupted in *Alk1*<sup>HEC-KO</sup> mice

When filtering the significantly dysregulated genes in EC from *Alk1*<sup>HEC-KO</sup> mice for angiocrine factors, *Wnt2*, *Wnt9b*, and R-spondin-3 (*Rspo3*) turned out to be significantly downregulated as validated by qPCR (Figure 6A,B). Moreover, the well-known LSEC angiokine *Bmp2*<sup>[32]</sup> was also significantly reduced in *Alk1*<sup>HEC-KO</sup> livers, whereas no changes in *hepatocyte growth factor* expression were found (Figure S8A). As angiocrine factors *Wnt2*, *Wnt9b*, and *Rspo3* are physiologically expressed in central vein EC and pericentral LSEC, we used ISH to confirm RNA-seq data and qPCR results. ISH revealed a significant loss of *Wnt2*, *Wnt9b*, and *Rspo3* in pericentral liver EC in *Alk1*<sup>HEC-KO</sup> mice (Figure 6C, Figure S8B). Based on these findings, we hypothesized that loss of pericentral angiocrine signaling in *Alk1*<sup>HEC-KO</sup> mice might cause disruption of metabolic liver zonation. Therefore, we performed immunofluorescence staining for zoned proteins, glutamine synthetase (GLUL) and arginase. GLUL expression was extinguished in *Alk1*<sup>HEC-KO</sup> livers, whereas arginase expression was extended, comprising pericentral hepatocytes (Figure 6D). Moreover, pericentral Rh Family B Glycoprotein expression was lost, whereas periportal GLS2 and HAL expression was increased (Figure S9A,B). Both aberrant sinusoidal endothelial differentiation and altered metabolic liver zonation patterns displayed a progressive phenotype with age, as supported by gradually increasing expression of EMCN and decreasing expression of LYVE1 and GLUL in the livers of 1-, 3- and 6-month-old *Alk1*<sup>HEC-KO</sup> mice (Figure S9C,D, Figure 6D, Figure 3C).

In a broader approach to decipher metabolic liver zonation in *Alk1*<sup>HEC-KO</sup> mice, we investigated the transcriptome of whole liver samples using RNA-seq.

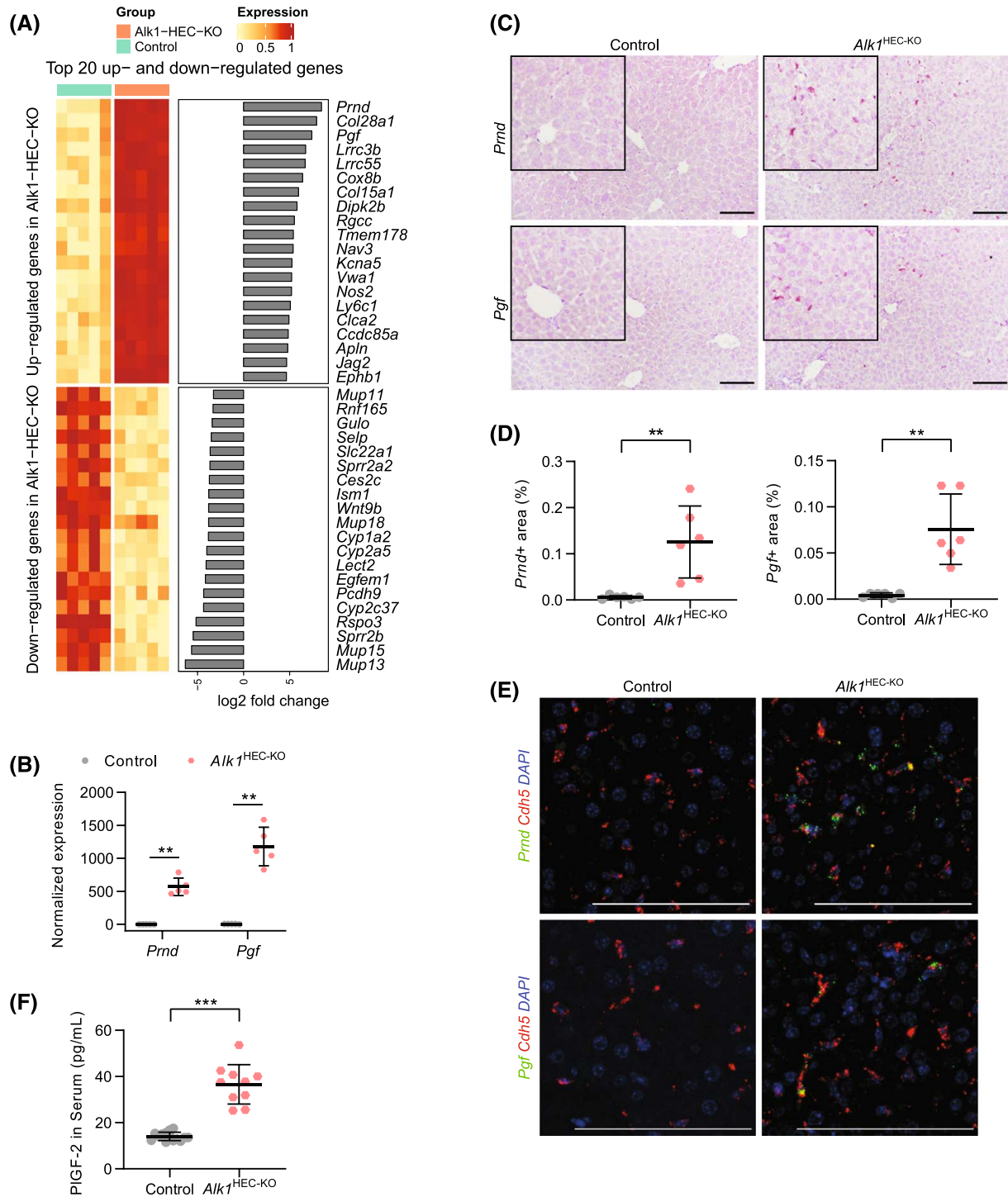


**FIGURE 5** Induction of proangiogenic factors including prion-like protein doppel (*Pmd*) and placental growth factor (*Pgf*) in *Alk1*-deficient mice. (A) Heatmap of top 20 upregulated and downregulated genes ordered by fold change in isolated hepatic endothelial RNA ( $n = 5$ ). (B) Quantitative polymerase chain reaction (qPCR) for identified proangiogenic factors *Pmd* and *Pgf* using isolated hepatic endothelial RNA ( $n = 5$ ). (C) In situ hybridization for *Pmd* and *Pgf* in mouse liver ( $n = 6$ ). (D) Quantification of in situ hybridizations in (C) ( $n = 6$ ). (E) Fluorescent in situ hybridization for *Pmd* or *Pgf* co-stained with *Cdh5*. (F) Enzyme-linked immunosorbent assay for placental growth factor (PIGF)-2 of blood serum ( $n = 8$ ). Scale bars: 100 μm. Error bars: mean with standard deviation. (B,D) Mann–Whitney  $U$  test; (F) Welch's  $t$  test. \*\* $p < 0.01$ ; \*\*\* $p < 0.001$ .

We found 48 genes that were significantly dysregulated in *Alk1*<sup>HEC-KO</sup> mice (Figure 6E, Figure S9E). Using publicly available single cell data sets providing zone-specific gene expression sets for nine layers of hepatocytes ranging from pericentral to periportal,<sup>[33]</sup>

we found that all significantly downregulated genes in whole liver samples from *Alk1*<sup>HEC-KO</sup> mice are physiologically found in the pericentral area revealing fundamental impairment of pericentral hepatocyte differentiation (Figure 6E). Notably, among the significantly

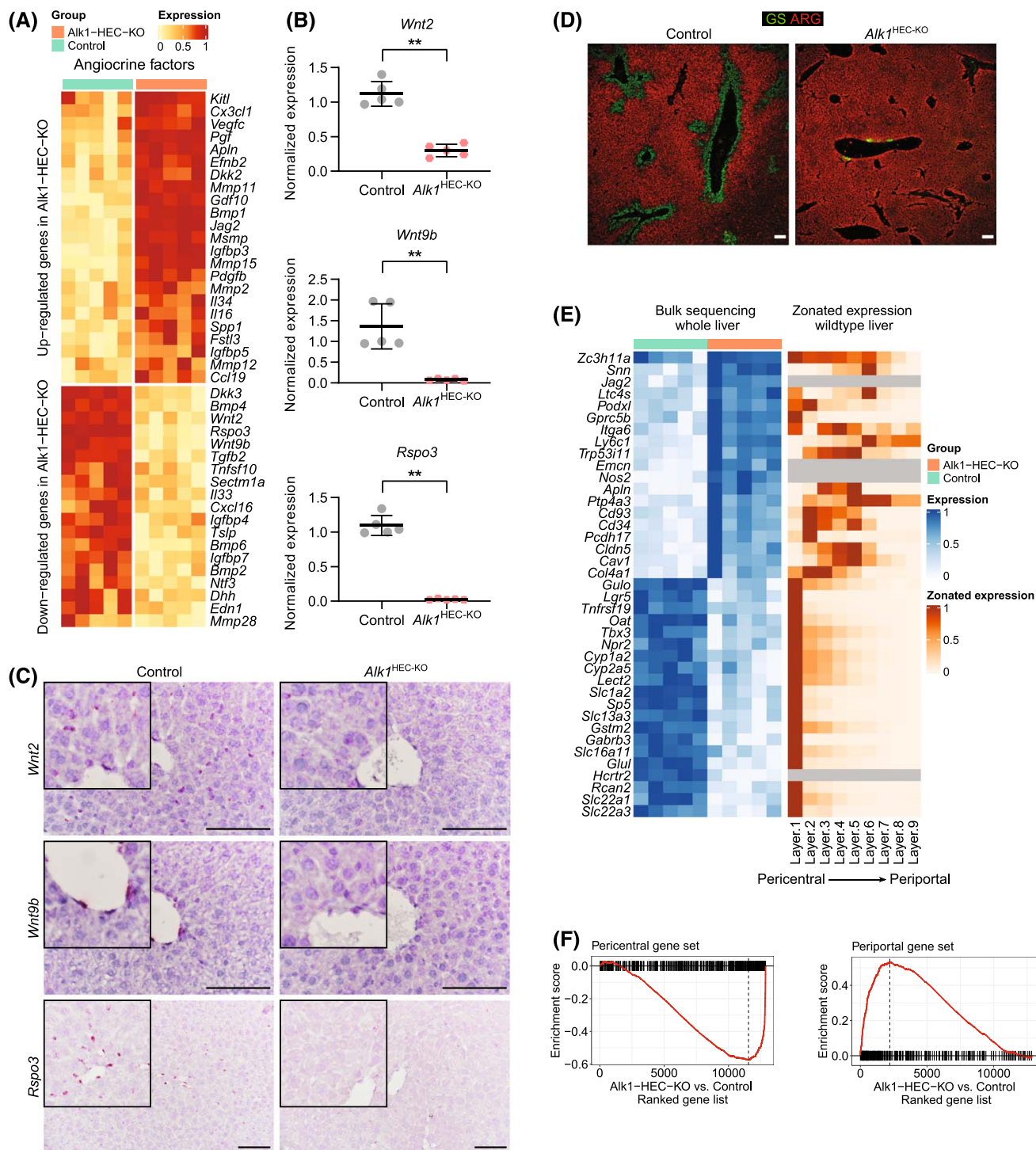


**FIGURE 6** Loss of endothelial Wnt factors correlates with disrupted metabolic zonation in *Alk1*<sup>HEC-KO</sup> mice. (A) Heatmap of significantly dysregulated angiocrine factors<sup>[23]</sup> in isolated hepatic endothelial RNA (*n* = 5). (B) Quantitative polymerase chain reaction (qPCR) for *Wnt2*, *Wnt9b*, and *R-spondin-3* (*Rspo3*) using isolated hepatic endothelial RNA (*n* = 5). (C) In situ hybridization for *Wnt2*, *Wnt9b*, and *Rspo3* in livers (*n* ≥ 4). (D) Immunofluorescent staining of glutamine synthetase (GLUL) and arginase (ARG) in livers (*n* = 5). (E) Heatmap of significantly dysregulated genes in whole liver RNA-sequencing (RNA-seq) data (*n* = 5). Genes are also annotated for the zone in which the genes are expressed in wild-type livers using published single cell RNA-seq data.<sup>[33]</sup> (F) Enrichment for pericentral (*p* < 0.001; normalized enrichment score [NES] = -2.97) and periportal (*p* < 0.001; NES = 2.57) genes<sup>[33]</sup> in whole liver RNA-seq data. Scale bars: 100 μm. Error bars: Mean with standard deviation. (B) Mann-Whitney *U* test. Wnt, portmanteau of the names Wingless and Int-1. \*\**p* < 0.01.

upregulated genes from whole liver bulk RNA-seq, we detected numerous genes associated with continuous endothelial differentiation and angiogenesis such as

*Apln*, *Emcn*, and *CD34* (Figure 6E). In another approach, we performed GSEA of our transcriptomic whole liver data using pericentral and periportal gene

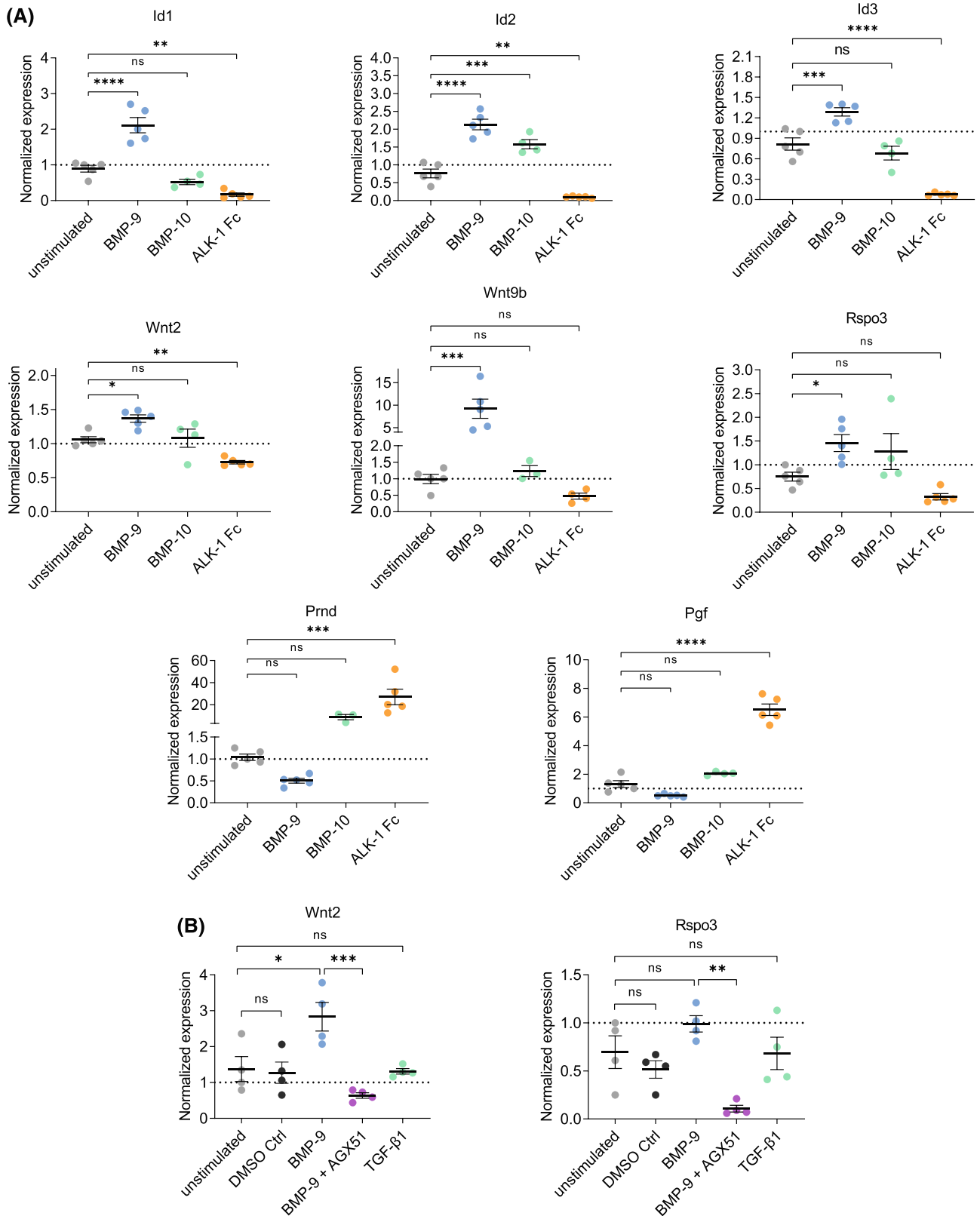


**FIGURE 7** ALK1 signaling enhances expression of Wnt factors and suppresses transcripts of prion-like protein doppel (*Pmd*) and placental growth factor (*Pgf*). (A) Wild-type (*Wt*) liver sinusoidal endothelial cells (LSEC) were stimulated *in vitro* with bone morphogenetic protein (BMP)-9, BMP-10, and ALK1-FC followed by quantitative polymerase chain reactions (qPCRs) for known ALK1 targets *Id1*, *Id2*, and *Id3*; Wnt factors *Wnt2*, *Wnt9b*, and R-spondin-3 (*Rspo3*); and proangiogenic factors *Prnd* and *Pgf* ( $n \geq 3$ ). (B) *Wt* LSEC were stimulated *in vitro* with BMP-9, BMP-9, Pan-ID antagonist AGX51, and transforming growth factor (TGF)- $\beta$ 1 followed by qPCRs for *Wnt2* and *Rspo3* ( $n = 4$ ). (A) One-way ANOVA followed by Dunnett's multiple comparisons test. (B) One-way ANOVA followed by Tukey's multiple comparisons test. Wnt, portmanteau of the names Wingless and Int-1. \* $p < 0.05$ ; \*\* $p < 0.01$ ; \*\*\* $p < 0.001$ ; \*\*\*\* $p < 0.0001$ .

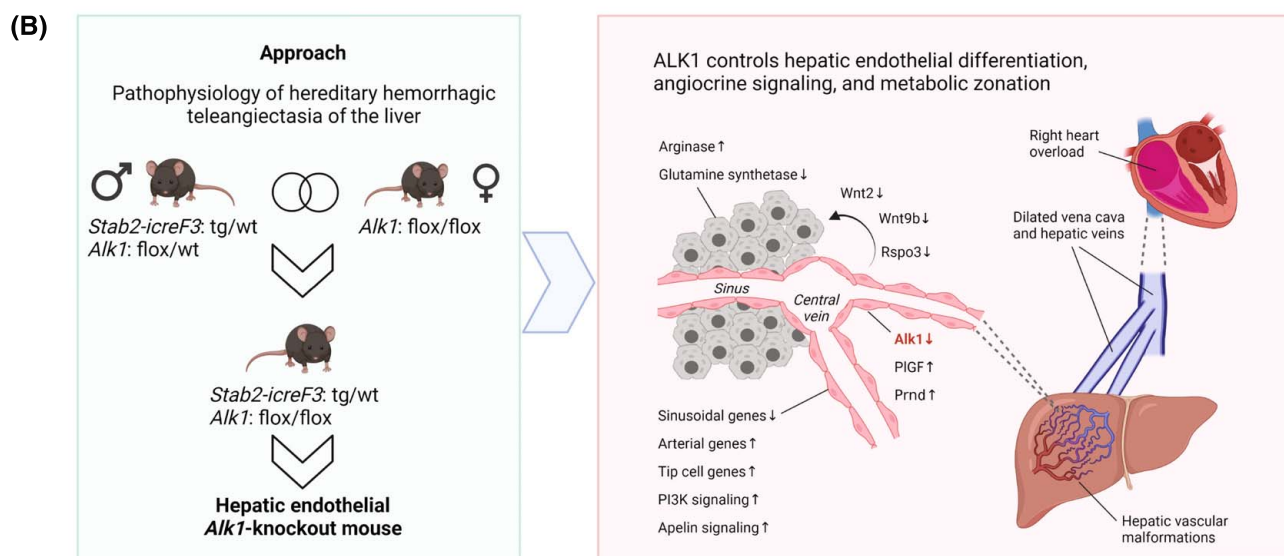
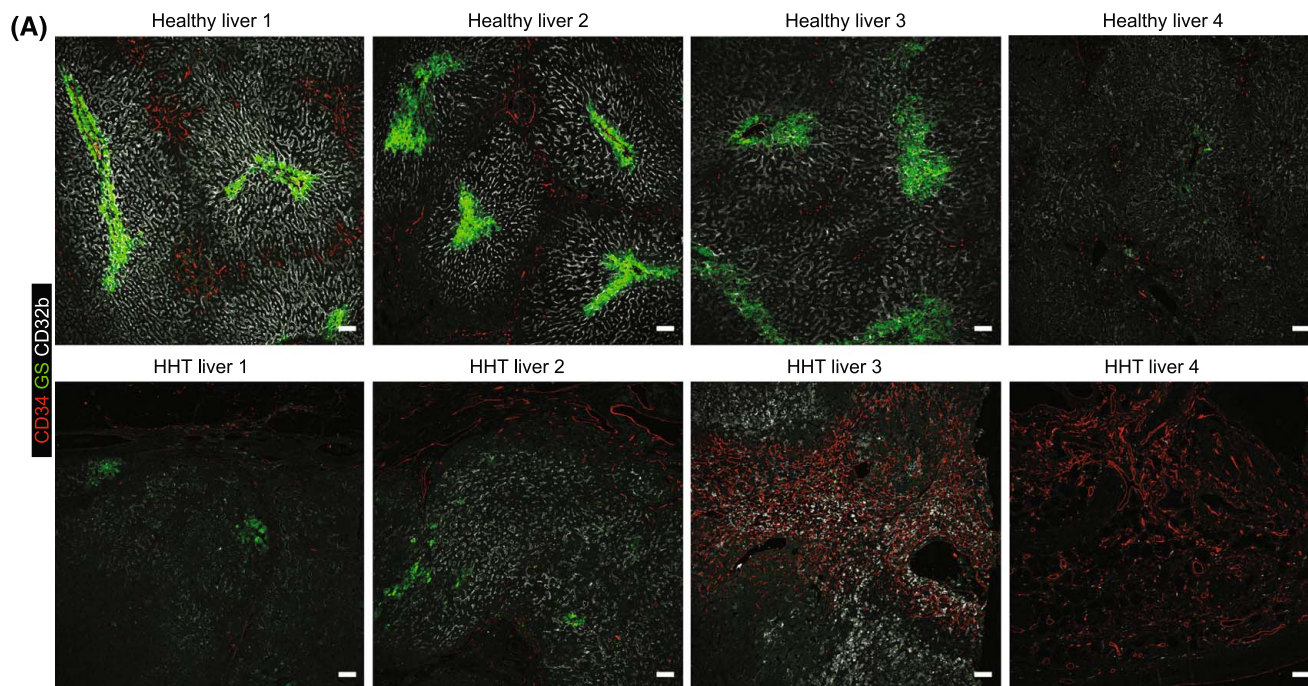


**FIGURE 8** Loss of metabolic zonation in human hereditary hemorrhagic telangiectasia (HHT) samples of the liver. (A) Immunofluorescence staining for CD34, CD32b, and glutamine synthetase (GLUL) in livers from patients with HHT and healthy individuals ( $n = 4$ ). Scale bars: 100  $\mu\text{m}$ . (B) Graphical summary of results in this study. Created with [BioRender.com](https://www.biorender.com).

sets defined by filtering published single cell RNA-seq data from Halpern et al.<sup>[33]</sup> GSEA confirmed the significant loss of pericentral genes and upregulation of periportal genes in *Alk1*<sup>HEC-KO</sup> mice (Figure 6F).

### ALK1 counter-regulates proangiogenic and organotypic angiocrine signaling in LSEC *in vitro*

In order to gain deeper mechanistic insight into the regulation of liver endothelial differentiation and

function, we performed *in vitro* experiments using murine LSEC isolated from wild-type mice. ALK1 signaling was induced by stimulation with BMP9 and BMP10, whereas inhibition was achieved using a soluble ALK1-FC fusion protein. Stimulation of LSEC with BMP9, and to a lesser extent with BMP10, caused upregulation of the major ALK1 downstream transcriptional targets, inhibitors of DNA binding (*ID*)1–3 (Figure 7), whereas inhibition of ALK1 signaling by *ID*1–3 genes. Wnt ligands *Wnt2*, *Wnt9b*, and *Rspo3* were similarly upregulated upon BMP9 stimulation,

whereas inhibition of ALK1 signaling caused significant mRNA overexpression of proangiogenic angiokine *Pgf* and vascular endothelial growth factor receptor (VEGFR)-2 coreceptor *Prnd* (Figure 7A). In addition, simultaneous stimulation of LSEC by BMP9 and by AGX51, an inhibitor of ID1–3 protein function, caused significant downregulation of *Wnt2* and *Rspo3* expression levels (Figure 7B). These data support the hypothesis that Wnt ligands and proangiogenic angiocrine factors *Prnd* and *Pgf* are regulated along the ALK1/ID1–3 signaling axis in hepatic EC.

### Hepatic angiodiversity and angiocrine functions are impaired in human HHT liver specimens

To confirm the findings in *Alk1*<sup>HEC-KO</sup> mice in human HHT, we analyzed liver samples of four patients with HHT (Table S2) who had undergone liver transplantation and compared them to archival, disease-free liver tissue. Human HHT livers exhibited an irregular vessel architecture within the liver parenchyma showing increased expression of continuous EC marker CD34 and reduced expression of LSEC marker CD32b (Figure 8A). Conversely, expression of GLUL was lost in human HHT liver samples (Figure 8A). These findings in human liver HHT thus well reflect the findings in our preclinical HHT mouse model.

## DISCUSSION

In this study, we have established a genetic mouse model to study HHT of the adult liver making use of *Stab2*-driven hepatic EC-specific knockout of *Acvr11* (*Alk1*<sup>HEC-KO</sup> mice). Hepatic endothelial *Alk1* deficiency caused replacement of organ-specific liver sinusoidal endothelial differentiation as well as impairment of large vessel differentiation by induction of angiogenesis as well as of arterialization and shunt formation in the hepatic vascular system (Figure 8B). In general, our findings indicate that ALK1 signaling is indispensable to induce and maintain vascular quiescence without interfering with organ-specific molecular mechanisms of microvascular angiodiversity or with macrovascular angiodiversity along the different segments of the vascular tree.

The hepatic vasculature of *Alk1*<sup>HEC-KO</sup> mice was irregular and showed effacement of the typical organ-specific angiodiversity. LSEC marker genes were lost and continuous EC marker genes such as EMCN and CD31 were induced, indicating aberrant sinusoidal endothelial differentiation. Disruption of sinusoidal differentiation often entails liver fibrosis. Hepatic endothelial *Alk1* deficiency indeed caused increased sinusoidal deposition of ECM proteins LAMC1 and

COL18A1; however, it did not result in full sinusoidal capillarization or subsequent liver fibrosis in our mouse model. It may be hypothesized that turbulences originating from the distorted slit-like sinusoids seen in the livers of *Alk1*<sup>HEC-KO</sup> mice could entail perisinusoidal ECM deposition. Our findings partly reflect the study by Desroches-Castan et al.; however, conflicting results have also been reported and may derive from confounding factors due to the different genetic backgrounds in the various models used.<sup>[11,15,16]</sup> Apart from disturbed blood vessel formation, we observed increased intrahepatic lymph vessels confirming the view that ALK1 does not only control blood but also lymph vessel angiogenesis.<sup>[34]</sup>

Apart from aberrant sinusoidal differentiation, hepatic endothelial *Alk1* deficiency impaired organ-specific angiocrine Wnt signaling (*Wnt2*, *Wnt9b*, *Rspo3*) by LSEC and central vein EC, causing disruption of metabolic liver zonation. Previously, we and others have shown that angiocrine Wnt signaling is necessary to establish metabolic liver zonation.<sup>[35,36]</sup> Nevertheless, the role of Wnt signaling in HHT has hitherto remained elusive, although metabolic liver zonation and angiocrine Wnt signaling have been shown to be disturbed in several pathological liver conditions including liver fibrosis/cirrhosis.<sup>[37,38]</sup> Furthermore, it is still a question of debate whether angiocrine Wnt signaling is decreased in these pathological conditions due to increased blood flow, reduced oxygen supply, altered signal cascades, or a combination thereof.<sup>[38]</sup>

On the other hand, hepatic endothelial *Alk1* deficiency induced de novo expression of angiogenic molecules *Prnd* and *Pgf*. *Prnd* and *Pgf* are both known to be involved in tumor angiogenesis in various tumors, including hepatocellular carcinoma.<sup>[39,40]</sup> Notably, both genes are physiologically expressed during liver development and are shut off around birth. PRND is a cell surface protein that stabilizes VEGFR-2 expression in the cell membrane and promotes angiogenesis. PRND has been reported to be inhibited using synthetic glycosaminoglycans in tumor angiogenesis.<sup>[41]</sup> Therefore, inhibition of PRND in HHT may be a promising approach to HHT therapy.

For PGF, diverse endothelial and nonendothelial functions have been described.<sup>[39]</sup> PGF is secreted from different cellular sources and binds to VEGFR-1 replacing vascular endothelial growth factor (VEGF)-A; increased availability of VEGF-A at VEGFR-2 then causes enhanced angiogenesis. In addition, the proangiogenic effect of PGF may be mediated by activating Neuropilin-1 and -2. Moreover, PGF is also able to induce other angiogenic factors including VEGF, fibroblast growth factor-2, and PDGF-B. On the other hand, PGF enhances proliferation, migration, and survival of macrophages that release angiogenic and lymphangiogenic factors. Notably, it has also been described that PGF promotes arterial vessel

differentiation.<sup>[42]</sup> In this respect, it has been a question of debate whether ALK1 signaling promotes arterial or venous vessel differentiation.<sup>[43]</sup> Our transcriptomic approach combined with published single cell data showed an increase of arterial transcripts. As the hepatic vasculature, however, is unique, variant responses to endothelial *Alk1* deficiency in the vasculature of different organs may be explained by inter-organ microvascular and macrovascular angiogenesis.

Imaging results of patients with HHT with liver involvement resemble the parenchymal enhancement pattern as seen upon CT of *Alk1*<sup>HEC-KO</sup> mice at 3 months of age.<sup>[44]</sup> In our HHT model, we observed functional shunting entailing volume overload of the right heart and dilatation of the vena cava. Our results, however, bear some limitations due to the CT technique used that does not allow for visualizing shunts directly and distinguishing between different types of shunts (arteriovenous, arterioportal, portovenous). Furthermore, *Alk1*<sup>HEC-KO</sup> mice exhibited neither dilated hepatic artery and dilated portal vein nor increased portal venous flow. Thus, we cannot easily reconcile that patients with HHT with liver involvement often display dilated hepatic artery and portal hypertension<sup>[44]</sup> because sonographic assessment of these parameters did not suggest portal hypertension caused by endothelial loss of *Alk1*. Time course differences might serve as an explanation because severe HHT in patients develops only slowly over many years, whereas our preclinical model was analyzed at 3 months of age shortly after maturation.

The remarkable similarities between our murine HHT model and the human disease confirm that *Alk1*<sup>HEC-KO</sup> mice represent a valuable tool to study HHT development in the liver and to develop and validate treatment strategies at different stages of disease development. At late stage HHT, heart failure is a severe complication due to liver shunting and volume overload which is also reflected by our HHT model. The pathophysiological processes leading to heart failure in HHT are clinically highly relevant and should be scrutinized in follow-up studies.

## AUTHOR CONTRIBUTIONS

Conceptualization, Christian David Schmid, Victor Olsavszky, Manuel Reinhart, Philipp-Sebastian Koch, Sergij Goerdts; investigation, Christian David Schmid, Victor Olsavszky, Manuel Reinhart, Vanessa Weyer, Felix A. Trogisch, Manuel Winkler, Sina W. Kürschner, Theresa Staniczek, Joerg Heineke, Kai Schledzewski, Jens Mittler, Karsten Richter; data curation, Christian David Schmid, Carsten Sticht; writing – original draft, Christian David Schmid, Victor Olsavszky, Philipp-Sebastian Koch, Sergij Goerdts; writing – review and editing, all authors; visualization, Christian David Schmid, Victor Olsavszky, Manuel Reinhart, Vanessa Weyer, Felix A. Trogisch; supervision, Cyrill Géraud,

Philipp-Sebastian Koch, Sergij Goerdts; funding acquisition, Victor Olsavszky, Manuel Winkler, Cyrill Géraud, Philipp-Sebastian Koch, Sergij Goerdts.

## ACKNOWLEDGMENTS

We thank Stephanie Riester, Hiltrud Schönhaber, Christof Dormann, Sina Göpel, and Carolina de la Torre for excellent technical support. We are grateful to Dr. Paul Oh (University of Florida College of Medicine) for providing *Alk1* floxed mice. Human tissues were kindly provided by the tissue biobank of the University Medical Center Mainz. Open Access funding enabled and organized by Projekt DEAL.

## FUNDING INFORMATION

The authors gratefully acknowledge the data storage service SDS@hd supported by the Ministry of Science, Research and the Arts Baden-Württemberg and the German Research Foundation (DFG) through grant INST 35/1314–1 FUGG and INST 35/1503–1 FUGG. This work was supported by the Deutsche Forschungsgemeinschaft, Germany (DFG, German Research Foundation), project numbers: 259332240 – RTG/GRK 2099; 394,046,768 – CRC/SFB 1366; 314,905,040 – CRC/SFB-TR 209; 413,262,200 – ICON/EB 187/8–1.

## CONFLICT OF INTEREST

The authors declare no conflict of interest.

## DATA AVAILABILITY STATEMENT

The RNA-seq data have been deposited in NCBI's Gene Expression Omnibus (GEO) and are accessible through GEO Series accession number GSE184748 (<https://www.ncbi.nlm.nih.gov/geo/query/acc.cgi?acc=GSE184748>); reviewer token: wrijakuqvbqxdqj.

## ORCID

Christian David Schmid  <https://orcid.org/0000-0002-4401-3394>

Victor Olsavszky  <https://orcid.org/0000-0001-6083-5534>

Manuel Winkler  <https://orcid.org/0000-0003-2415-9350>

Johannes Hoffmann  <https://orcid.org/0000-0002-2774-7847>

Philipp-Sebastian Koch  <https://orcid.org/0000-0001-5236-0516>

## REFERENCES

1. Shovlin CL, Guttmacher AE, Buscarini E, Faughnan ME, Hyland RH, Westermann CJJ, et al. Diagnostic criteria for hereditary hemorrhagic telangiectasia (Rendu-Osler-Weber syndrome). *Am J Med Genet.* 2000;91:66–7.
2. Dakeishi M, Shioya T, Wada Y, Shindo T, Otaka K, Manabe M, et al. Genetic epidemiology of hereditary hemorrhagic telangiectasia in a local community in the northern part of Japan. *Hum Mutat.* 2002;19:140–8.

3. Porteous ME, Burn J, Proctor SJ. Hereditary haemorrhagic telangiectasia: a clinical analysis. *J Med Genet.* 1992;29:527–30.
4. Pierucci P, Lenato GM, Suppressa P, Lastella P, Triggiani V, Valerio R, et al. A long diagnostic delay in patients with hereditary haemorrhagic telangiectasia: a questionnaire-based retrospective study. *Orphanet J Rare Dis.* 2012;7:33.
5. Johnson DW, Berg JN, Baldwin MA, Gallione CJ, Marondel I, Yoon SJ, et al. Mutations in the activin receptor-like kinase 1 gene in hereditary haemorrhagic telangiectasia type 2. *Nat Genet.* 1996;13:189–95.
6. McAllister KA, Grogg KM, Johnson DW, Gallione CJ, Baldwin MA, Jackson CE, et al. Endoglin, a TGF-beta binding protein of endothelial cells, is the gene for hereditary haemorrhagic telangiectasia type 1. *Nat Genet.* 1994;8:345–51.
7. Sabbà C, Pasculli G, Lenato GM, Suppressa P, Lastella P, Memeo M, et al. Hereditary hemorrhagic telangiectasia: clinical features in ENG and ALK1 mutation carriers. *J Thromb Haemost.* 2007;5:1149–57.
8. Larrivée B, Prahst C, Gordon E, del Toro R, Mathivet T, Duarte A, et al. ALK1 signaling inhibits angiogenesis by cooperating with the notch pathway. *Dev Cell.* 2012;22:489–500.
9. Cai J, Pardali E, Sánchez-Duffhues G, ten Dijke P. BMP signaling in vascular diseases. *FEBS Lett.* 2012;586:1993–2002.
10. Bonnardel J, T'Jonck W, Gaublomme D, Browaeys R, Scott CL, Martens L, et al. Stellate cells, hepatocytes, and endothelial cells imprint the kupffer cell identity on monocytes colonizing the liver macrophage niche. *Immunity.* 2019;51:638–54.e9.
11. Breitkopf-Heinlein K, Meyer C, König C, Gaitantzi H, Addante A, Thomas M, et al. BMP-9 interferes with liver regeneration and promotes liver fibrosis. *Gut.* 2017;66:939–54.
12. David L, Mallet C, Mazerbourg S, Feige JJ, Bailly S. Identification of BMP9 and BMP10 as functional activators of the orphan activin receptor-like kinase 1 (ALK1) in endothelial cells. *Blood.* 2007;109:1953–61.
13. Scharpfenecker M, van Dinther M, Liu Z, van Bezooijen RL, Zhao Q, Pukac L, et al. BMP-9 signals via ALK1 and inhibits bFGF-induced endothelial cell proliferation and VEGF-stimulated angiogenesis. *J Cell Sci.* 2007;120:964–72.
14. Massagué J. TGFβ signalling in context. *Nat Rev Mol Cell Biol.* 2012;13:616–30.
15. Desroches-Castan A, Tillet E, Ricard N, Ouarné M, Mallet C, Belmudes L, et al. Bone morphogenetic protein 9 is a paracrine factor controlling liver sinusoidal endothelial cell fenestration and protecting against hepatic fibrosis. *Hepatology.* 2019;70:1392–408.
16. Desroches-Castan A, Tillet E, Ricard N, Ouarné M, Mallet C, Feige JJ, et al. Differential consequences of Bmp9 deletion on sinusoidal endothelial cell differentiation and liver fibrosis in 129/Ola and C57BL/6 mice. *Cell.* 2019;8:E1079.
17. Tual-Chalot S, Oh SP, Arthur HM. Mouse models of hereditary hemorrhagic telangiectasia: recent advances and future challenges. *Front Genet.* 2015;6:25.
18. Aird WC. Phenotypic heterogeneity of the endothelium: I. Structure, function, and mechanisms. *Circ Res.* 2007;100:158–73.
19. Rockey DC, Weymouth N, Shi Z. Smooth muscle α actin (Acta2) and myofibroblast function during hepatic wound healing. *PLoS One.* 2013;8:e77166.
20. Jakab M, Augustin HG. Understanding angiodiversity: insights from single cell biology. *Development.* 2020;147:dev146621.
21. Koch PS, Lee KH, Goerdts S, Augustin HG. Angiodiversity and organotypic functions of sinusoidal endothelial cells. *Angiogenesis.* 2021;24:289–310.
22. Geraud C, Koch PS, Zierow J, Klapproth K, Busch K, Olsavszky V, et al. GATA4-dependent organ-specific endothelial differentiation controls liver development and embryonic hematopoiesis. *J Clin Invest.* 2017;127:1099–114.
23. Winkler M, Staniczek T, Kürschner SW, Schmid CD, Schönhaber H, Cordero J, et al. Endothelial GATA4 controls liver fibrosis and regeneration by preventing a pathogenic switch in angiocrine signaling. *J Hepatol.* 2021;74:380–93.
24. World Medical Association. World Medical Association Declaration of Helsinki: ethical principles for medical research involving human subjects. *JAMA.* 2013;310:2191–4.
25. Heil J, Olsavszky V, Busch K, Klapproth K, de la Torre C, Sticht C, et al. Bone marrow sinusoidal endothelium controls terminal erythroid differentiation and reticulocyte maturation. *Nat Commun.* 2021;12:6963.
26. Park SO, Lee YJ, Seki T, Hong KH, Fliess N, Jiang Z, et al. ALK5- and TGFBR2-independent role of ALK1 in the pathogenesis of hereditary hemorrhagic telangiectasia type 2. *Blood.* 2008;111:633–42.
27. Kalucka J, de Rooij LPMH, Goveia J, Rohlenova K, Dumas SJ, Meta E, et al. Single-cell transcriptome atlas of murine endothelial cells. *Cell.* 2020;180:764–79.e20.
28. Halpern KB, Shenhav R, Massalha H, Toth B, Egozi A, Massasa EE, et al. Paired-cell sequencing enables spatial gene expression mapping of liver endothelial cells. *Nat Biotechnol.* 2018;36:962–70.
29. Ola R, Dubrac A, Han J, Zhang F, Fang JS, Larrivée B, et al. PI3 kinase inhibition improves vascular malformations in mouse models of hereditary haemorrhagic telangiectasia. *Nat Commun.* 2016;7:13650.
30. Chen W, Xia P, Wang H, Tu J, Liang X, Zhang X, et al. The endothelial tip-stalk cell selection and shuffling during angiogenesis. *J Cell Commun Signal.* 2019;13:291–301.
31. Aspalter IM, Gordon E, Dubrac A, Ragab A, Narloch J, Vizán P, et al. Alk1 and Alk5 inhibition by Nrp1 controls vascular sprouting downstream of Notch. *Nat Commun.* 2015;6:7264.
32. Koch PS, Olsavszky V, Ulbrich F, Sticht C, Demory A, Leibing T, et al. Angiocrine Bmp2 signaling in murine liver controls normal iron homeostasis. *Blood.* 2017;129:415–9.
33. Halpern KB, Shenhav R, Matcovitch-Natan O, Toth B, Lemze D, Golan M, et al. Single-cell spatial reconstruction reveals global division of labour in the mammalian liver. *Nature.* 2017;542:352–6.
34. Niessen K, Zhang G, Ridgway JB, Chen H, Yan M. ALK1 signaling regulates early postnatal lymphatic vessel development. *Blood.* 2010;115:1654–61.
35. Leibing T, Geraud C, Augustin I, Boutros M, Augustin HG, Okun JG, et al. Angiocrine Wnt signaling controls liver growth and metabolic maturation in mice. *Hepatology.* 2018;68:707–22.
36. Wang B, Zhao L, Fish M, Logan CY, Nusse R. Self-renewing diploid Axin2(+) cells fuel homeostatic renewal of the liver. *Nature.* 2015;524:180–5.
37. D'Ambrosio R, Aghemo A, Rumi MG, Ronchi G, Donato MF, Paradis V, et al. A morphometric and immunohistochemical study to assess the benefit of a sustained virological response in hepatitis C virus patients with cirrhosis. *Hepatology.* 2012;56:532–43.
38. Soto-Gutierrez A, Gough A, Verneti LA, Taylor D, Monga SP. Pre-clinical and clinical investigations of metabolic zonation in liver diseases: the potential of microphysiology systems. *Exp Biol Med (Maywood).* 2017;242:1605–16.
39. Albonici L, Giganti MG, Modesti A, Manzari V, Bei R. Multifaceted role of the placental growth factor (PlGF) in the antitumor immune response and cancer progression. *Int J Mol Sci.* 2019;20:2970.
40. Coulon S, Heindryckx F, Geerts A, Steenkiste CV, Colle I, Vlierbergh HV. Angiogenesis in chronic liver disease and its complications. *Liver Int.* 2011;31:146–62.
41. Al-Hilal TA, Chung SW, Choi JU, Alam F, Park J, Kim SW, et al. Targeting prion-like protein doppel selectively suppresses tumor angiogenesis. *J Clin Invest.* 2016;126:1251–66.
42. Pipp F, Heil M, Issbrücker K, Ziegelhoeffer T, Martin S, van den Heuvel J, et al. VEGFR-1-selective VEGF homologue PlGF is



- arteriogenic: evidence for a monocyte-mediated mechanism. *Circ Res.* 2003;92:378–85.
43. Rochon ER, Wright DS, Schubert MM, Roman BL. Context-specific interactions between Notch and ALK1 cannot explain ALK1-associated arteriovenous malformations. *Cardiovasc Res.* 2015;107:143–52.
  44. Wu JS, Saluja S, Garcia-Tsao G, Chong A, Henderson KJ, White RI. Liver involvement in hereditary hemorrhagic telangiectasia: CT and clinical findings do not correlate in symptomatic patients. *AJR Am J Roentgenol.* 2006;187:W399–405.

**How to cite this article:** Schmid CD, Olsavszky V, Reinhart M, Weyer V, Trogisch FA, Sticht C, et al. ALK1 controls hepatic vessel formation, angiodiversity, and angiocrine functions in hereditary hemorrhagic telangiectasia of the liver. *Hepatology.* 2023;77:1211–1227. <https://doi.org/10.1002/hep.32641>